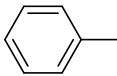
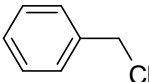
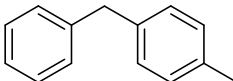
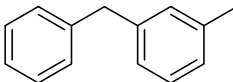
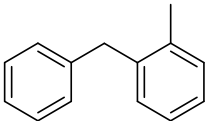


Supporting Information for

Stability and activity of Zn/MCM-41 materials in the alkylation of toluene with benzyl chloride: microwave irradiation vs continuous flow

Paola M. Carraro ¹, Bruna S. Goldani ², Diego S. Alves ², A. Gabriel Sathicq ³, Griselda A. Eimer ¹, Gustavo P. Romanelli ^{3,4} and Rafael Luque ^{5,6,*}

The size of the reagent and product molecules was determined after optimization of their conformation. The conformation of the compounds was drawn by means of the “model build” modulus available in HyperChem 5.0. Each molecular structure was firstly pre-optimized with the Molecular Mechanics Force Field (MM+) procedure, and the resulting geometry was further refined by means of the semi-empirical method PM3 (Parametric Method-3). A gradient norm limit of 0.01 kcal Å⁻¹ was chosen.

	Diameter [nm]	Area [Å ²]	Area (grid) [Å ²]	Volume [Å ³]
	0.585	249.06	268.21	382.58
	0.586	269.55	291.66	425.90
	1.099	363.19	402.36	641.91
	0.996	361.57	399.59	642.51
	0.937	348.80	392.18	634.13

The infrared spectra for all samples are shown in Figure S1. All literature described main bands for MCM-41 are present in the synthesized materials [1]. Two bands at ca. 1085 and 1238 cm⁻¹ are associated with internal and external asymmetric Si-O stretching modes, while bands at 800 and 460 cm⁻¹ can be assigned to Si-O-Si stretching and bending of Si-O bonds, respectively.

Furthermore, an adsorption band around 960 cm⁻¹ is noted [2-3]. Thus, the presence of bands around 960-965 cm⁻¹ has been generally assigned to Si-O-metal (where metal = Al and Zn) vibrations [4-5]. However, pure silica MCM-41 also exhibits such band around 960 cm⁻¹, attributed to the lattice defect of MCM-41 framework. Consequently, this band can be inferred in terms of the overlapping of signals from silanol groups and Si-O-Zn vibrations.

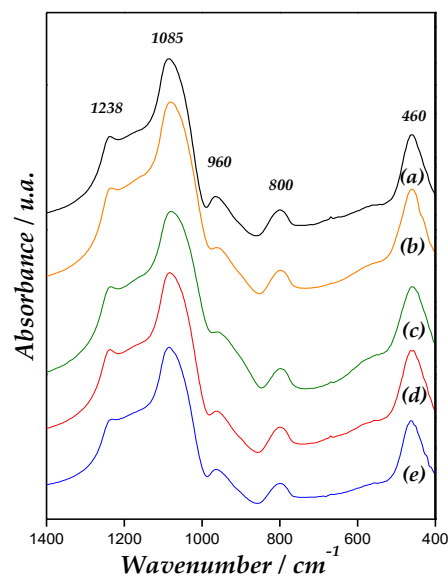


Figure S1. FT-IR spectra in the 400-1400 cm^{-1} range of (a) MCM-41, (b) Zn/MCM-41(1), (c) Zn/MCM-41(2.5), (d) Zn/MCM-41(10) and (e) Zn/MCM-41(15) catalysts.

1. Eimer, G. A.; Casuscelli, S. G.; Chanquia, C. M.; Elías, V.; Crivello, M. E.; Herrero, E. R. The influence of Ti-loading on the acid behavior and on the catalytic efficiency of mesoporous Ti-MCM-41 molecular sieves. *Catal. Today* **2008**, 133–135, 639–646. doi:10.1016/j.cattod.2007.12.096
2. Kamitsos, E.I.; Patsis, A.P.; Kordas, G. Infrared-reflectance spectra of heat-treated sol-gel-derived silica. *Phys. Rev. B* **1993**, 48, 12499. 10.1103/PhysRevB.48.12499
3. Eimer, G.; Casuscelli, S.; Ghione, G.; Crivello, M.; Herrero, E. Synthesis, characterization and selective oxidation properties of Ti-containing mesoporous catalysts. *Appl. Catal. A* **2006**, 298, 232-242. 10.1016/j.apcata.2005.10.006
4. Palani, A.; Gokulakrishnan, N.; Palanichamy, M.; Pandurangan, A. Transesterification of Dimethyl Carbonate with Diethyl Carbonate over Al-Zn-MCM-41 and Al-MCM-41 Molecular Sieves. *Appl. Catal. A* **2006**, 304, 152-158. 10.1016/j.apcata.2006.02.036.
5. Vaschetto, E. G.; Pecchi, G. A.; Casuscelli, S. G.; Eimer G. A. Nature of the active sites in Al-MCM-41 nano-structured catalysts for the selective rearrangement of cyclohexanone oxime toward ϵ -caprolactam. *Micropor. Mesopor. Mater.* **2014**, 200, 110-116. 10.1016/j.micromeso.2014.08.030

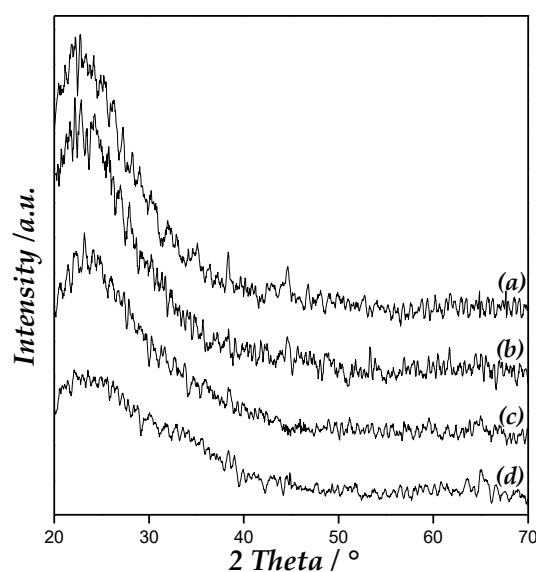


Figure S2. High-angle XRD patterns of (a) Zn/MCM-41(1), (b) Zn/MCM-41(2.5), (c) Zn/MCM-41(10) and (d) Zn/MCM-41(15).

Materials and Methods

Catalyst preparation

Samples were synthesized with cetyltrimethylammonium bromide (CTAB, Merck, 99%), tetraethoxysilane (TEOS, Aldrich, 98%), sodium hydroxide (NaOH) and zinc-nitrate ($\text{Zn}(\text{NO}_3)_2 \cdot 6\text{H}_2\text{O}$, Anedra, 99.2 %).

The pure siliceous mesoporous material (MCM-41) was prepared following the pathway reported by Elías et al. [6]. Molar rates: sodium hydroxide/Silicon = 0.50, CTAB/ Silicon = 0.12, H_2O / Silicon = 132. The mixture was vigorously stirred for 4 h at room temperature and then for 3 h at 70 °C in a closed flask. The final solid was recovered by filtration, and was further washed and dried at 60 °C overnight. To obtain the MCM-41 support, the solid was calcined firstly under N_2 flow and then under air at 500 °C for 6 h at a heating rate of 2 °C/min.

Zn/MCM-41 catalysts were prepared by the wet impregnation method using zinc nitrate salt as precursor. 0.75 g of silica, previously calcined at 500 °C for 10 h, was added to 37 mL of aqueous solution of $\text{Zn}(\text{NO}_3)_2 \cdot 6\text{H}_2\text{O}$ with a concentration corresponding to the desired metallic loading. Then, the water was slowly evaporated in a rot evaporator at 50 °C. The obtained material was dried at 60 °C and then calcined at 500 °C for 9 h. Four impregnations were made using different percentages of theoretical zinc, and the samples were named as Zn/MCM-41(x), where x corresponds to 1, 2.5, 10 and 15 wt%.

Characterization

The quantity of Zn in the obtained materials was determined by inductively coupled plasma - atomic emission spectroscopy (ICP - AES) using a spectrophotometer VISTA-MPX CCD Simultaneous ICP-OES-VARIAN. The samples were previously digested with HF and HNO_3 .

The structural characterization of the samples was performed by X-ray powder diffraction (XRD) using $\text{Cu K}\alpha$ radiation ($\lambda=1.5418 \text{ \AA}$), measured with a PANalytical X'Pert PRO diffractometer in the range of 2θ from 1.5 to 7° and from 10 to 80°.

The textural characterization was carried out by N_2 adsorption- desorption isotherms at -196 °C (N_2 with 99.999 % purity) in Micromeritics ASAP 2000. The samples were previously vacuum-degassed at 300 °C for 12 h. From the N_2 adsorption-desorption data obtained for each catalyst and support, the specific surface was calculated by the Brunauer-Emmett-Teller (S_{BET}) method [7] and the total pore volume (V_{TP}) was obtained by the Gurvich rule [8]. The primary mesopore volume (V_{MP}) was estimated by the α -plot method as reported by Jaroniec et al. [9] using macroporous silica gel LiChrospher Si-1000 as the reference adsorbent. The pore size distributions (PSD) were determined by the nonlocal density functional theory (NLDFT), for SiO_2 cylindrical pores in the adsorption branches [10]. Moreover, the solids were analyzed by transmission electron microscopy (TEM) with a JOEL JEM-1200 EX II, working voltage: 120 kV. A small drop of the dispersion (sample in water-ethanol solution 50%) was deposited on a copper grid and then evaporated in air at room temperature.

The morphology of the materials was observed by scanning electron microscopy (SEM) using a JEOL JSM-6380 LV, and the acceleration voltage was 20 kV. Gold coverage was applied to make the samples conductive.

The diffuse reflectance ultraviolet-visible (UV-Vis DRS) spectra in absorbance mode were recorded using a Jasco 650 spectrometer with an integrating sphere in the wavelength range of 200-900 nm.

Fourier transform infrared (FT-IR) data were performed on Nicolet iS10 FTIR spectrometer (Thermo Scientific) with the wave range of 400 and 4000 cm^{-1} . The samples were pressed into a self-supported wafer at room temperature using KBr. Afterwards, in order to determine the concentration of Lewis and Bronsted acidic sites, FT-IR adsorption of pyridine were carried out. Self-supported pellets of the samples (~20 mg and 13 mm of diameter) were

disposed in a thermostated cell with CaF₂ windows and evacuated at 400 °C for 7 h under vacuum. After cooling to room temperature (RT), the spectrum of each sample was registered. Subsequently, the solid wafer was saturated with pyridine vapors (Sintorgan, 99% purity) up to a pressure of 46 mm Hg at RT for 12 h. The IR spectrum for each sample was obtained before and after pyridine adsorption and desorption by evacuation for 1 h at 50, 100 and 200 °C. The difference spectrum was obtained by subtracting the background spectrum preliminarily recorded.

For quantitative analysis, the numbers of Lewis acid sites (amount of adsorbed pyridine (mmolPy/gcat)) were calculated on the basis of the relationship reported by Emeis [11] from the integration of Lewis bands evaluated in the spectra registered at 200 °C, using the integrated molar extinction coefficient, which is independent of the catalysts or strength of the sites.

3.3. Catalytic experiments

The alkylation of toluene with benzyl chloride was conducted in a microwave tube. One mL toluene, 0.1 mL benzyl chloride and 12.5 mg catalyst were heated at 120 °C for 15 min. Samples were taken every 5 min, filtered off and analysed using a HP5890 Series II Gas Chromatograph (60 mL min⁻¹ N₂ carrier flow, 20 psi column top head pressure) fitted with a capillary HP-101 column (25 m x 0.2 mm x 0.2 mm) and a flame ionization detector (FID). All calculations including activities and selectivities have been based on the use of benzyl chloride as limiting reagent.

The reusability experiments were carried out as follows: 1 mL Tol, 0.1 mL BC and 12.5 mg catalyst were introduced to a microwave tube and heated at 120 °C. Five minutes after reaching a quantitative conversion, the mixture was filtered off in order to separate the catalysts, and this was washed with toluene and kept in an oven at 100 °C for 1 h prior to its use in the next alkylation reaction. For their reutilization, the catalyst was regenerated at 400 °C for 2 h to test.

When flow chemistry was used, the alkylation of Tol with BC was carried out in a 100 mL flask. Ninety mL Tol, 9 mL BC and 110 mg catalyst were taken up to 120 °C at different times (0.4 mL/min.). Samples were collected at defined times, filtered and analyzed employing an HP5890 Series II Gas Chromatograph (60 mL min⁻¹ nitrogen flow, 20 psi column top head pressure) with a capillary HP-101 column (25 m x 0.2 mm x 0.2 mm) and a FID detector.

6. Elías, V.; Crivello, M.; Herrero, E.; Casuscelli, S.; Eimer, G. Some considerations to optimize the synthesis procedure and the structural quality of mesostructured silicas. *J. Non-Cryst. Solids* **2009**, *355*, 1269-1273. 10.1016/j.jnoncrysol.2009.04.019
7. Brunauer, S.; Emmett, P.H.; Teller, E. Adsorption of Gases in Multimolecular Layers. *J. Am. Chem. Soc.* 1938, *60*, 309-339. 10.1021/ja01269a023
8. Rouquerol, F.; Rouquerol, J.; Sing, K. In: Adsorption by powders and porous solids, principles, methodology and application. Academic Press, 1999.
9. Jaroniec, M.; Kruck, M.; Olivier, J. Standard Nitrogen Adsorption Data for Characterization of Nanoporous Silicas. *Langmuir* 1999, *15*, 5410-5442. 10.1021/la990136e
10. Ravikovitch, P.I.; Neimark, A.V. Characterization of nanoporous materials from adsorption and desorption isotherms. *Colloids Sur., A* 2001, *11*, 187-188. 10.1016/S0927-7757(01)00614-8
11. Emeis, C.A. Determination of Integrated Molar Extinction Coefficients for Infrared Absorption Bands of Pyridine Adsorbed on Solid Acid Catalysts. *J. Catal.* 1993, *141*, 347-354. 10.1006/jcat.1993.1145